Summer 6-1-2018

# Magnetic reconnection and Blandford-Znajek process around rotating black holes

David Garofalo
*Physics Department Kennesaw State University*, dgarofal@kennesaw.edu

Chandra B. Singh
*Tel Aviv University*

Elisabete M. de Gouveia Dal Pino
*University of Sao Paulo*

MNRAS **000**, 1–7 (2018) Preprint 24 May 2018 Compiled using MNRAS LATEX style file v3.0

# Magnetic reconnection and Blandford-Znajek process around rotating black holes

Chandra B. Singh,[1,2,4]★ David Garofalo,[3,4]† and Elisabete M. de Gouveia Dal Pino[2]
[1] *The Raymond and Beverly Sackler School of Physics and Astronomy, Tel Aviv University, Tel Aviv 69978, Israel*
[2] *Department of Astronomy (IAG-USP), University of Sao Paulo, Sao Paulo, Brazil*
[3] *Department of Physics, Kennesaw State University, Marietta GA 30060, USA*
[4] *Equal first authors*

Accepted XXX. Received YYY; in original form ZZZ

**ABSTRACT**
We provide a semi-analytic comparison between the Blandford-Znajek (BZ) and the magnetic reconnection power for accreting black holes in the curved spacetime of a rotating black hole. Our main result is that for a realistic range of astrophysical parameters, the reconnection power may compete with the BZ power. The field lines anchored close to or on the black hole usually evolve to open field lines in general relativistic magnetohydrodynamic (GRMHD) simulations. The BZ power is dependent on the black hole spin while magnetic reconnection power is independent of it for the near force-free magnetic configuration with open field lines adopted in our theoretical study. This has obvious consequences for the time evolution of such systems particularly in the context of black hole X-ray binary state transitions. Our results provide analytical justification of the results obtained in GRMHD simulations.

**Key words:** accretion, accretion discs – black hole physics – galaxies: jets – X-rays: binaries

## 1 INTRODUCTION

Outflows and jets are ubiquitous in various astrophysical sources ranging from young stellar objects to black holes. Usually relativistic jets are observed in X-ray binaries (XRBs), active galactic nuclei (AGN) and gamma-ray bursts (GRBs) which are likely to have black holes as central compact objects (Begelman, Blandford & Rees 1984). There are likely to be different mechanisms working in connection with origin, acceleration and collimation of jets, namely, thermal pressure, radiation pressure and magnetohydrodynamics (MHD) processes. These mechanisms may be either at work in different sources or in the same source at different scales (e.g., Beskin 2010). Based on the role of magnetic fields, there are two popular models: the jet is powered by accretion via a magneto-centrifugal mechanism known as the Blandford-Payne process (Blandford & Payne 1982) and the Blandford-Znajek mechanism (Blandford & Znajek 1977; Lee, Wijers & Brown 2000 and references therein) wherein the rotation of black hole powers the jet through the magnetic lines anchored in its horizon. During the accretion process, large scale magnetic field lines are likely to be dragged along with the accreting matter and field lines may accumulate and become dynamically important with the ram pressure of the accretion flow balanced by magnetic pressure, a scenario referred to as Magnetically Arrested Disk (MAD)(Narayan, Igumenshchev & Abramowicz 2003; Bisnovatyi-Kogan & Ruzmaikin 1974). Pseudo-Newtonian (Igumenshchev 2008) as well as general relativistic (GR) MHD (Tchekhovskoy, Narayan, McKinney 2011 ; McKinney, Tchekhovskoy, Blandford 2012) simulations have confirmed such highly efficient accretion flow. The topology of field lines can also play important roles: quadrupole loops, for instance, can lead to less powerful and episodic jets compared to dipolar ones (Beckwith, Hawley & Krolik 2008).

Along with these processes, magnetic reconnection may also play a role in extracting energy efficiently from the black hole surroundings (de Gouveia Dal Pino & Lazarian 2005; de Gouveia Dal Pino, Piovezan & Kadowaki 2010; Kadowaki, de Gouveia Dal Pino & Singh 2015; Singh, de Gouveia Dal Pino & Kadowaki 2015) and in powering jets (e.g., Giannios, Uzdensky & Begelman 2009; Zhang & Yan 2011; Singh, Mizuno & de Gouveia Dal Pino 2016). Fast magnetic reconnection can occur independently of microscopic plasma properties in presence of turbulence (Lazarian & Vishniac 1999) and has been tested numerically in three dimensional (3D) MHD Newtonian (Kowal et al. 2009; Kowal, de Gouveia Dal Pino & Lazarian

★ E-mail: chandratalk@gmail.com (CBS)
† E-mail : dgarofal@kennesaw.edu (DG)

2012) as well as special relativistic MHD regimes (Takamoto, Inoue, Lazarian 2015). Even from initial weak noise of velocity fluctuations, the process of reconnection can generate turbulence which in turn may drive it faster ( Beresnyak 2017; Kowal et al. 2017). First-order Fermi acceleration can occur in magnetically dominated environments due to fast magnetic reconnection (de Gouveia Dal Pino & Lazarian 2005; Drury 2012) and this process has been also tested successfully both via MHD ( Kowal, de Gouveia Dal Pino & Lazarian 2011; Kowal, de Gouveia Dal Pino & Lazarian 2012; del Valle, de Gouveia Dal Pino & Lazarian 2016; Beresnyak & Li 2016) and kinetic PIC simulations (e.g., Drake et al. 2006; Zenitani & Hoshino 2008; Sironi & Spitkovsky 2014; Guo et al. 2014; Werner et al. 2016; Werner & Uzdensky 2017).

Frame dragging effects of rotating black holes can lead to complicated magnetic current sheet structures and occurrence of magnetic reconnection can accelerate plasma (Koide & Arai 2008; Karas, Kopa'cek & Kunneriath 2012). Pseudo-Newtonian (Machida & Matsumoto 2003; Igumenshchev 2009), force-free (Parfrey, Giannios & Beloborodov 2015) and GRMHD simulations (Hirose et al. 2004; Ball et al. 2016, 2018; Dexter et al. 2014) have confirmed the polarity inversion of field lines and formation of magnetic reconnection sites around spinning black holes. The regions of high current density are possible locations of high magnetic dissipation hence the reconnection sites and can lead to acceleration of non-thermal electrons and X-ray and gamma-ray flaring. Taking into account small scale magnetic flux loops in presence of turbulence, axisymmetric force free simulations have shown that relativistic jets can be driven by magnetic reconnection and may be responsible for hard X-ray emission (e.g. Parfrey, Giannios & Beloborodov 2015), as predicted in de Gouveia Dal Pino & Lazarian (2005) using a Newtonian approach. In another work dealing with large scale magnetic fields, Semenov, Dyadechkin & Heyn (2014) showed that reconnection cuts flux tubes and causes the ejection of plasmoids that mimic a particle-like Penrose mechanism as it carries extracted black hole rotational energy. Long term evolution of GRMHD simulations of MAD or magnetically choked accretion flow (MCAF) by McKinney, Tchekhovskoy, Blandford (2012) for black hole of spin 0.9375 and poloidal field with flipping type showed that reconnection of field lines in the inner region of accretion flows around black holes can drive a transient outflow which is as powerful as a steady BZ jet (Dexter et al. 2014). This can be associated with change of states in black hole X-ray binaries. Further continuing the same set of GRMHD simulations, O'Riordan, Pe'er & McKinney (2016) showed that for a population of thermal electrons, during launching of the transient plasmoid, when BZ jet is quenched, the ratio of gamma-ray luminosity to X-ray luminosity becomes less than 1 while in the case of the steady BZ jet it remains greater than 1.

Beskin & Zheltoukhov (2013), using a force free analytical solution under the assumption of axisymmetric and stationary flow, could explain the profile of the angular velocity of the field lines which were obtained from the 3D GRMHD simulations of McKinney, Tchekhovskoy, Blandford (2012). Motivated by the success of this analytical study to explain the numerical results, we here apply fast reconnection theory to address the properties that are seen in the simulations of transient jets with respect to the black hole spin. Our goal is to analytically explore the contribution of curved spacetime and black hole spin to fast magnetic reconnection in order to try to shed light on some of the results seen in numerical simulations of black hole accretion. To accomplish this we develop a solution that to a first approximation is removed from force-free magnetic field configuration. In section 2 we present the equations and expressions relevant to build a force-free black hole magnetosphere. In section 3 the magnetic reconnection power and BZ power are discussed depending upon various accretion parameters and black hole properties. Section 4 deals with summary and conclusions of our work.

## 2 A FORCE-FREE KERR BLACK HOLE MAGNETOSPHERE

In this section we develop a general relativistic expression for the magnetic reconnection power from a rotating black hole. Our background spacetime is that of Kerr which we describe using Boyer-Lindquist coordinates $(t, r, \theta, \phi)$ [1] which are well known to be singular at the null horizon:

$$dS^2 = -(1-2Mr/\rho^2)dt^2 - (4Marsin^2\theta/\rho^2)dtd\phi + (\Sigma^2/\rho^2)sin^2\theta d\phi^2 + (\rho^2/\Delta)dr^2 + \rho^2 d\theta^2, \quad (1)$$

with $\rho^2 = r^2 + a^2 r_g^2 cos^2\theta$, $\Delta = r^2 - 2r_g r + r_g^2 a^2$ and $\Sigma^2 = (r^2 + a^2 r_g^2)^2 - a^2 r_g^2 \Delta sin^2\theta$ where $a$, $M$ and $r_g = GM/c^2$ are the angular momentum per unit mass, mass and gravitational radius of the black hole respectively. Here $G$ and $c$ are the gravitational constant and speed of light, respectively. The associated contravariant metric tensors are given as follows : $g^{tt} = -\frac{\Sigma^2 c^2}{\rho^2 \Delta}$, $g^{rr} = \frac{\Delta}{\rho^2}$, $g^{\theta\theta} = \frac{1}{\rho^2}$, $g^{\phi\phi} = \frac{\Delta - a^2 r_g^2 sin^2\theta}{\rho^2 \Delta sin^2\theta}$ and $g^{t\phi} = -\frac{2arr_g}{\rho^2\Delta}$ (Chandrasekhar 1983).

The singular nature of the horizon is not a problem for our analysis since we are interested in exploring a region of spacetime outside both the black hole and the accretion disk, a hypersurface in $r$, $\theta$ spanning the radial location $r$ of 10 to $50r_g$, and a coordinate $\theta$ range of 30° to 45 °. We let $a$ vary across the entire possible range. In addition to the assumption of a background Kerr spacetime, we will assume that the magnetosphere is to first order force-free. Although such a configuration is by construction non-dissipative, we will explore the possible consequences of a magnetosphere that evolves away from force-freeness and how this evolution affects reconnection. This force-free approach is taken because of the simplicity introduced in the system of equations, which allows for the development of a family of analytic solutions for the magnetic flux around the black hole. Besides, a force- free configuration is naturally expected in the coronal regions around black-hole accretion disk system

[1] We note that the polar coordinate $\theta$ varies between 0 (on the rotation axis) and $\pi/2$ (on the equator), and the azimuthal coordinate $\phi$ between 0 and $2\pi$.

(e.g. Hirose et al. 2004). The equations that govern the system are as follows. The force-free condition is

$$F_{ab}j^b = 0, \tag{2}$$

where $F_{ab}$ is the Faraday tensor and $j^b$ is the current 4-vector. In terms of the vector potential we have

$$F_{ab} = A_{b,a} - A_{a,b}. \tag{3}$$

As in Blandford & Znajek (1977), the force-free condition allows to define the following function $\omega$ as

$$\omega = -\frac{A_{t,r}}{A_{\phi,r}} = \frac{A_{t,\theta}}{A_{\phi,\theta}}, \tag{4}$$

where the right hand side involves radial and angular partial derivatives of the vector potential one-form components. We assume a steady-state configuration and axisymmetry, which specifies the gauge. The importance of the force-free assumption in developing an analytic solution is due to the function in equation (4), which can be thought of as the angular velocity of the field lines for which there is physical intuition that we can appeal to. We will determine this function by assuming that the magnetic flux is frozen into the accretion disk plasma in the equatorial plane so that $\omega$ reduces to the Keplerian function at $\theta = 90°$. In addition, we assume there is a tenuous plasma in order to define a velocity field and impose the zero proper electric field condition

$$F_{ab}U^b = 0, \tag{5}$$

where $U^b$ is the 4-velocity and components are taken from equation (13) of Yokosawa, Ishizuka & Yabuki (1991) as follows:

$$U^t = \frac{\Sigma^2}{\rho^2\Delta}, \quad U^r = -\frac{[2r_g r(r^2+a^2r_g^2)]^{1/2}}{\rho^2}, \quad U^\theta = 0, \quad U^\phi = \frac{2ar_g r}{\rho^2\Delta}. \tag{6}$$

The invariant magnetic flux, $A_\phi$ has been prescribed as (Blandford & Znajek 1977)

$$A_\phi = br(1-cos\theta). \tag{7}$$

This gives the magnetic flux as a function of $r$ and $\theta$. It is a typical solution for paraboloidal magnetic field configuration and seen in GRMHD simulations as well (e.g., McKinney & Narayan 2007).

Since our solution corresponds to force-free regime around a black hole, the Alfven speed is of the order of the light speed $c$ (e.g. de Gouveia Dal Pino & Lazarian 2005, O'Riordan, Pe'er & McKinney 2016). Our primary goal will be to anchor the conversation in a general relativistic analog of magnetic energy density. For that purpose we evaluate the invariant $F_{ab}F^{ab}$ which is obtained as follows

$$F_{ab}F^{ab} = 2\alpha B_r^2 g^{\theta\theta} + 2\beta B_\theta^2 g^{rr} + 2\gamma B_\phi^2 + 4\delta B_\theta B_\phi g^{rr} + 4\xi B_r B_\phi g^{\theta\theta}, \tag{8}$$

where $B$'s are the magnetic field components using the vector potential given in equation (7) and can be expressed as $B_r = -brsin\theta$ and $B_\theta = b(1-cos\theta)$. Here,

$$\alpha = g^{\phi\phi} - (2g^{t\phi} - g^{tt})(U^\phi/U^t)^2,$$

$$\beta = g^{\phi\phi} - 2g^{t\phi}(U^\phi/U^t) + g^{tt}(U^\phi/U^t)^2,$$

$$\gamma = g^{rr}g^{\theta\theta} + g^{tt}g^{rr}(U^\theta/U^t)^2 + g^{tt}g^{\theta\theta}(U^r/U^t)^2,$$

$$\delta = g^{t\phi}(U^\theta/U^t) - g^{tt}[U^\theta U^\phi/(U^t)^2],$$

$$\xi = g^{t\phi}(U^r/U^t) - g^{tt}[U^r U^\phi/(U^t)^2].$$

Note that the magnetic field components in the Boyer Lindquist frame ($B^a$) are obtained from $g^{ac}g^{bd}F_{ab}$. Therefore, the background Kerr metric appears in physical magnetic field components as well as in the magnetic energy density $F_{ab}F^{ab}$. It is important to emphasize that $F_{ab}F^{ab}$ is therefore expressed fully in the background Kerr metric. It is the contribution of that parameter for magnetic reconnection that we are most interested in and has been used in equation (11) as well as equation (12) .

From the simulations we know that our prespription is approximately force-free in the coronal region close to funnel wall region like around 30° from the rotation axis such that beyond a certain threshold value of 45°, the solution is no longer force-free. As a result, we limit our analytic explorations to regions in the coronal region with angles smaller than 45°. The disk region is thus outside the scope of our work.

In order to determine the coefficient $b$ appearing in equation (7), we consider the equilibrium condition between ram pressure of freely-falling matter and magnetic pressure on the equatorial plane $\theta = 90°$ and at $10r_g$ for non-rotating black hole ($a = 0$) which can be expressed as

$$\frac{F_{ab}F^{ab}}{16\pi} = \frac{GM}{r^2}\frac{\dot{M}}{2\pi r v_{in}}. \tag{9}$$

Here, $v_{in}$ being the infall velocity of the matter which can be certain fraction of free-fall velocity $v_{ff} = -\sqrt{2GM/r}$. The corresponding four velocity components are given by $(U^t)_{eq} = [r/(r-2r_g)]$, $(U^r)_{eq} = \sqrt{2r_g/r}$, $(U^\theta)_{eq} = (U^\phi)_{eq} = 0$. The magnetic field components are expressed as $(B_r)_{eq} = -br$ and $(B_\theta)_{eq} = b$. The contravariant metric tensors become $(g^{tt})_{eq} = -(1-\frac{2r_g}{r})c^2$, $(g^{rr})_{eq} = 1-\frac{2r_g}{r}$, $(g^{\theta\theta})_{eq} = (g^{\phi\phi})_{eq} = \frac{1}{r^2}$ and $(g^{t\phi})_{eq} = 0$. The subscript $eq$ indicates the corresponding expressions for the accretion flow in the equatorial plane. As a result of our calculations,

$$\mathrm{b} = \left[\frac{4GM\dot{M}}{v_{in}(r-r_g)[2+r^2-\frac{2c^2r_g}{r}(1+r^2)(r-2r_g)^2]}\right]^{1/2}. \tag{10}$$

Following expressions in Singh, de Gouveia Dal Pino & Kadowaki (2015) the magnetic reconnection power release from magnetic discon-

tinuity in the freely falling plasma around the black hole is

$$P_{MB} = \frac{F_{ab}F^{ab}}{16\pi} v_{rec} 4\pi L_X R_X, \quad (11)$$

where $v_{rec}$ is the reconnection velocity and is typically a few percent of the Alfven speed (Lazarian & Vishniac 1999; Takamoto, Inoue, Lazarian 2015; Beresnyak 2017; Kowal et al. 2017), and $L_X$ and $R_X$ are the reconnection region length and the inner radius location of the current sheet, respectively. For our comparative study, BZ power is given by (Meier 2012)

$$P_{BZ} = \frac{F_{ab}F^{ab}}{32} r_g^2 c a^2. \quad (12)$$

## 3 RESULTS

In this section we evaluate the dependence of the reconnection power on $r$, $\theta$, $a$, mass accretion rate $\dot{M}$ and $M$. We then determine the parameters that minimize and maximize the reconnection power and compare it to the Blandford- Znajek power extracted from black hole rotation.

### 3.1 Radial dependence

We begin by evaluating equation (11) as a function of $r$. For this initial analysis, the parameters are fixed in the following way: we adopt a characteristic value of $a = 0.9375$ and $M = 10M_\odot$(solar masses) based on the results of the GRMHD simulations (Dexter et al. 2014). To calculate the reconnection power, we considered polar angles in the range $\theta = 30° - 45°$, radial inflow velocities ($v_{in}$) as 1% - 10% of the free-fall velocity $v_{ff}$ (Narayan, Igumenshchev & Abramowicz 2003), mass accretion rates $\dot{M}$ in the range of 0.05 to 0.0005 of the Eddington value and the length of the current sheet $L_X$ between 0.1 and 1 times the radial location $R_X$. The reconnection velocity $v_{rec}$ = 1% - 5% of $c$. Top panel of Fig. 1 shows the upper and lower bounds of the reconnection power for this parametric space. The upper curve corresponds to the maximum values of the parameters above, while the lower curve corresponds to the minimum values (except $v_{in}$, for which the lower value corresponds to the upper curve). The reconnection power in both curves is smaller at 10 gravitational radii ($r_g$) and increases outward by about order of unity at $50r_g$.

### 3.2 Angular dependence

In the bottom panel of Fig. 1 we report the results of a similar analysis for the reconnection power, obtained by fixing $r$ at 50 $r_g$, and adopting the values for the remaining parameters that maximized the power in the upper panel, namely a 1% of $v_{ff}$, a 0.05 Eddington accretion rate, a current sheet that is equal in length to the radial location or to its coordinate value, $v_{rec}$ as 5% of $c$, and letting the polar angle $\theta$ to vary. In other words, we explore the reconnection power along an arc. The result is displayed in the upper curve. The lower curve reflects the angular dependence of the power for fixed radial location of 10 $r_g$, 0.0005 Eddington accretion

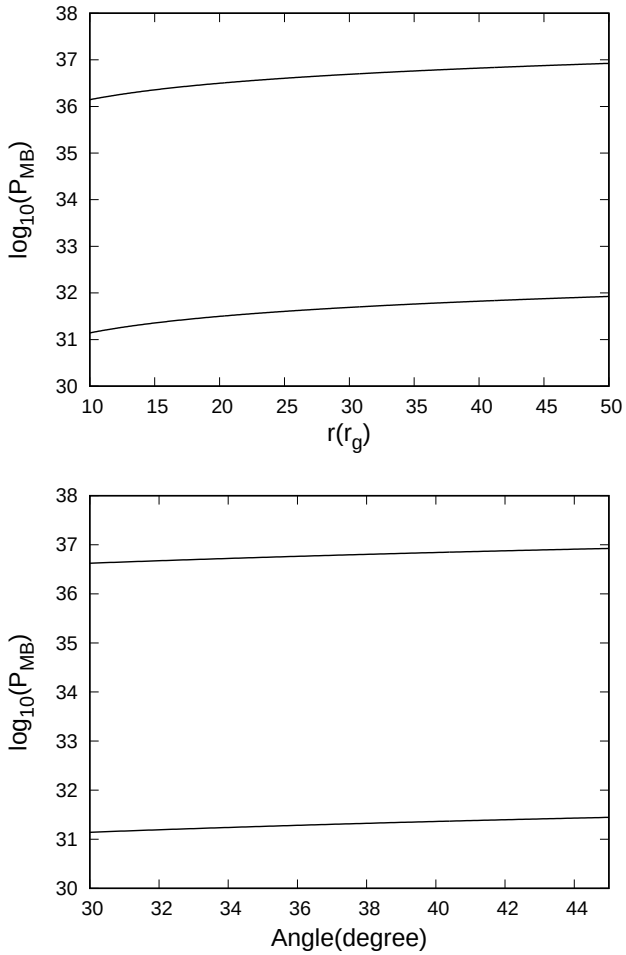


**Figure 1.** Magnetic reconnection power $P_{MB}$ (in units of erg/s) versus radial location $r$ (in units of gravitational radius, $r_g$) (top panel), and versus angle $\theta$ (in units of degree) (bottom panel). The curves give upper and lower bounds for the $P_{MB}$ calculated for a parametric space (see text for details).

rate, $v_{rec}$ as 1% of c, current sheet length $L_X$ about 10% of the radial location value $R_X$ and $v_{in}$ as 10% of $v_{ff}$. Similar to the radial dependence, the angular range introduces less than an order of magnitude difference in reconnection power, the greater power occurring closer to the equatorial plane. We have constrained our angular range to be compatible with the results of numerical simulations that suggest that force-freeness does not extend to higher angular regions (O'Riordan, Pe'er & McKinney 2016).

### 3.3 Mass accretion rate dependence

In top panel of Fig. 2, we explore the dependence of the reconnection power on the mass accretion rate which varies from 0.0005 to 0.05 Eddington rate for $M = 10\ M_\odot$ and $a = 0.9375$. We find about a two order of magnitude difference as the accretion rate approaches the theoretical boundary between an advection dominated accretion flow and a radiatively efficient thin disk at about a few percent Eddington rate (Meier 2012). The upper and lower curves are evaluated for 50 and $10r_g$, respectively, and the remaining parameters are the same as upper panel of Fig. 2. In the bottom

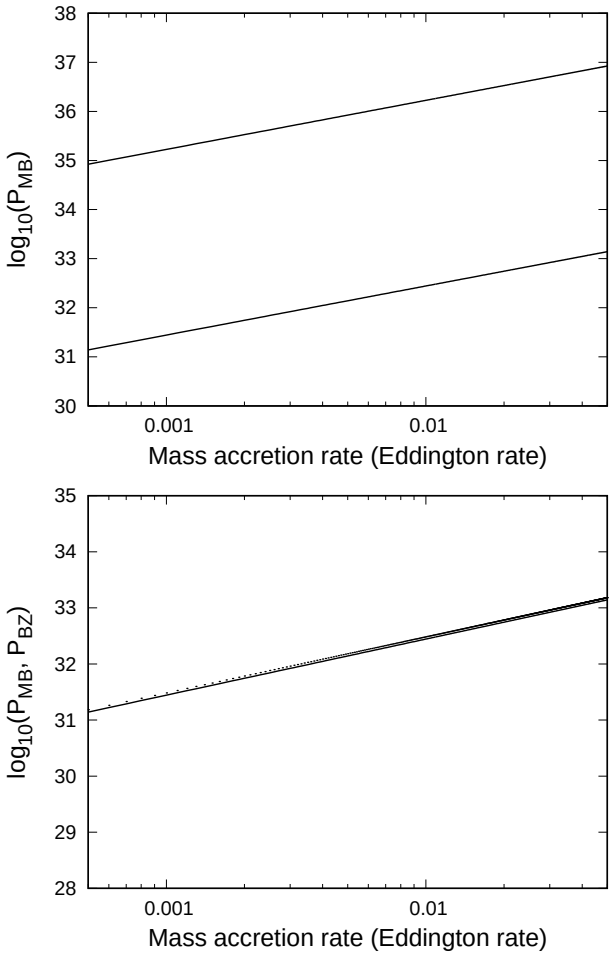


**Figure 2.** Magnetic reconnection power $P_{MB}$ (in units of erg/s) versus mass accretion rate $\dot{M}$ (in units of Eddington rate) (top panel), and $P_{MB}$ (solid line) and Blandford-Znajek power $P_{BZ}$ (dotted line) versus mass accretion rate (in units of Eddington rate) (bottom panel) (see text for details).

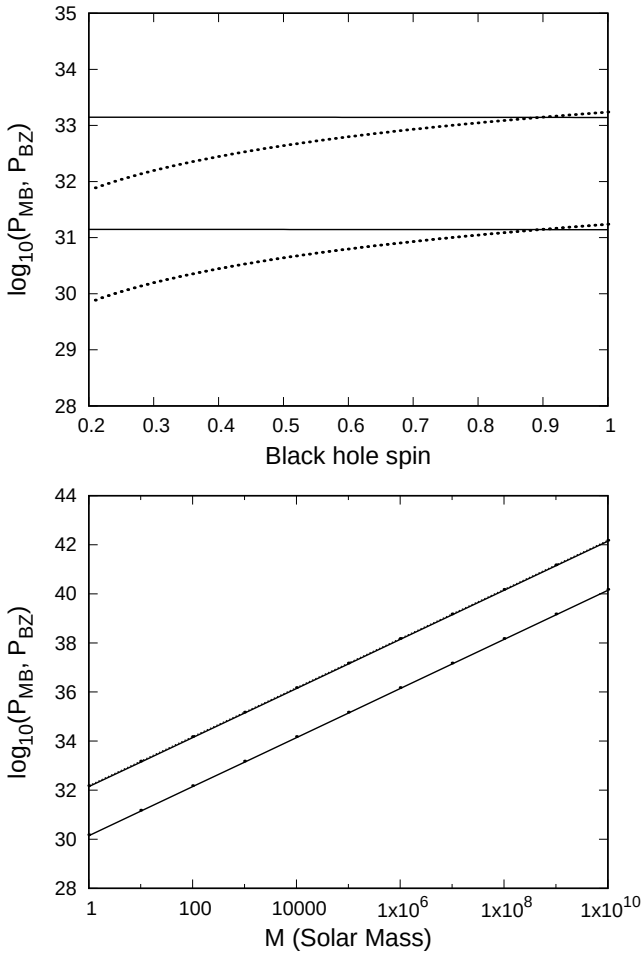


**Figure 3.** Magnetic reconnection power $P_{MB}$ (solid lines) and Blandford-Znajek power $P_{BZ}$ (dotted lines) plotted against black hole spin $a$ (top panel) and black hole mass $M$ (bottom panel). The two curves coincide in the bottom panel (see text for details).

panel of Fig. 2, we compare the reconnection power with the Blandford-Znajek power(BZ) evaluated for the parameter values r = $10r_g$, $\theta = 30$, $v_{rec}$ as 1% of c, current sheet length $L_X$ about 10% of the radial location value $R_X$ and $v_{in}$ as 10% of $v_{ff}$. This illustrates the important result that both powers can be comparable for reasonable parameters.

### 3.4 Spin dependence

Top panel of Fig. 3 depicts the upper and lower limits for the BZ power and the reconnection power versus the black hole spin $a$, for the parametric space: r = $10r_g$, $\theta = 30$, $\dot{M}$ = 0.0005-0.05 Eddington rate, $v_{rec}$ as 1% of c, $L_X$ about 10% of $R_X$, and $v_{in}$ as 10% of $v_{ff}$. Perhaps surprisingly, we find the effect of black hole spin $a$ to be negligible for the reconnection power, while the BZ power strongly depends on $a$, the magnetic reconnection appears to be independent of it. Usually in GRMHD simulations, field lines attain open configuration close to black hole (e.g. Dexter et al. 2014, O'Riordan, Pe'er & McKinney 2016), we have also adopted similar configuration in force-free regime for our analytical study. Our current results revealing a near independence of the magnetic reconnection power with black hole spin is compatible with that of GRMHD simulations (Dexter et al. 2014).

We would like to highlight that the slopes of curves representing magnetic reconnection and BZ powers are same in case of dependence on mass accretion rate and black hole mass dependence due to scale invariance nature of theory however symmetry is broken for black hole spin.

### 3.5 Mass dependence

In bottom panel of Fig. 3, we explore the maximum and minimum reconnection power as a function of the black hole of spin $a = 0.9375$ and mass which we allow to vary over 10 orders of magnitude from 1 to $10^{10}$ solar masses, sweeping the same parametric space as in upper panel. This analysis shows that the conditions that maximize the reconnection power also make the reconnection power competitive with the Blandford-Znajek power, the latter being evaluated at the same dimensionless spin value $a$ = 0.9375 . This is not surprising as we have imposed a balance of forces in the magnetosphere which naturally scales with the black hole mass. This result is also similar to

the one found in (Kadowaki, de Gouveia Dal Pino & Singh 2015; Singh, de Gouveia Dal Pino & Kadowaki 2015) in the evaluation of the magnetic reconnection power around black holes neglecting GR effects.

### 3.6 Astrophysical implications

The takeaway message from our plots is that reconnection power can compete with the BZ power for a reasonable range of astrophysical parameters. Since reconnection events take energy away from magnetic form, non-negligible reconnection makes it difficult for steady-state BZ jets. As conditions arise that make the Alfven velocity increase, the reconnection power begins to compete with the BZ power. Magnetic reconnection partially destroys the field, but such that the field comes back, producing the observed hysteresis of the jet and the conditions that effectively terminate the field to cause the transition to the soft state in XRBs. In greater detail, as the accretion rate increases, both the reconnection power as well as the magnetic field will increase so there is competition between these two effects with the accretion rate contributing to greater BZ power but reconnection power contributing to destroying large scale field and thus weakening BZ power. On the other hand increase in B-field also contributes to a decrease in accretion rate so it might come natural in this overall competition to see the hysteresis behaviour. Such time dependent phenomena need detailed study as a separate work.

## 4 SUMMARY AND CONCLUSIONS

We have performed a general relativistic semi-analytic exploration of magnetic reconnection around rotating black holes. We determined a range of reconnection power based on a fiducial astrophysical parameter space. While not strictly taking into account an exact force-free magnetic configuration, we were interested in developing an analytic solution for a black hole magnetosphere aiming at understanding where magnetic reconnection might develop or at least constitute an effective energy release mechanism near black holes. However, since it is difficult to develop non force-free solutions analytically, our strategy has allowed us a complete analytic solution by considering slight modifications to the force-free solution and in a way that has allowed compatibility with the numerical simulations. The magnetic reconnection power release is minimum close to the black hole and near spin axis in the coronal region. It is likely to increase in strength with increase in mass accretion rate. Our main result is that reconnection power may compete or even dominate the BZ power. This raises the question of the time evolution of such systems and we have pointed out a reconnection-based picture of the evolution and eventual disappearance of the BZ jet, suggesting it can provide a possible explanation for state transitions in black hole XRBs.

Following are the main highlights of our work in agreement with simulation works (e.g. Dexter et al. 2014):

1. The power available from both the BZ mechanism and fast magnetic reconnection is comparable for rapidly rotating black holes and same range of mass accretion rates.

2. The BZ mechanism is dependent on the black hole spin while the fast magnetic reconnection process in the proximity of the black hole seems to be independent of the black hole spin.

3. The BZ process can be quenched in the presence of fast magnetic reconnection. This may occur due to the destruction of large scale magnetic fields following magnetic reconnection events. Therefore, one can argue that the state transitions of stellar mass black hole accretion disk systems could be triggered by this process (as suggested in e.g. de Gouveia Dal Pino, Piovezan & Kadowaki 2010, Kadowaki, de Gouveia Dal Pino & Singh 2015).

In brief, we mainly used the conditions available in simulation set up regarding accretion flow and black hole properties in the analytical theory of BZ and magnetic reconnection so that we can give theoretical interpretation of phenomena seen in simulation results.

## ACKNOWLEDGEMENTS

CBS acknowledges support from the Brazilian agency FAPESP (grant 2013/09065-8) and was also supported by the I-Core centre of excellence of the CHE-ISF. EMGDP acknowledges partial support from FAPESP (2013/10559-5) and CnPq (306598/2009-4) grants.

## REFERENCES

Ball D., Ozel F., Pslatis D., Chan C.-K. Chan, 2016, ApJ, 826, 77
Ball D., Ozel F., Pslatis D., Chan C.-K. Chan, Sironi L., 2018, ApJ, 853, 184
Beckwith K., Hawley J.F., Krolik J.H., 2008, ApJ, 678, 1180
Begelman M.C., Blandford R.D., Rees M.J., 1984, Rev. Mod. Phys., 56, 255
Beresnyak A., 2017, ApJ, 834, 47
Beresnyak A., Li H., 2016, ApJ, 819, 90
Beskin V.S., 2010, Phys. U., 53, 1199
Beskin V.S., Zheltoukhov A.A., 2013, Azh, 39, 215
Bisnovatyi-Kogan G.S., Ruzmaikin A.A., 1974, Ap&SS, 28, 45
Blandford R.D., Payne D.G., 1982, MNRAS, 199, 883
Blandford R.D., Znajek R.L., 1977, MNRAS, 179, 433
Chandrasekhar S., 1983, The Mathematical Theory of Black Holes. Oxford Univ. Press, Oxford
de Gouveia dal Pino E. M., Lazarian A., 2005, A&A, 441, 845
de Gouveia dal Pino E. M., Piovezan P.P., Kadowaki L.H.S., 2010, A&A, 518, A5
del Valle M.V., de Gouveia dal Pino E. M., Kowal G., 2016, MNRAS, 463, 4331
Dexter J., McKinney J.C., Markoff S., Tchekhovskoy A., 2014, MNRAS, 440, 2185
Drake J. F., Swisdak M., Che H., Shay M.A., 2006, Nature, 443, 553
Drury L.O' C., 2012, MNRAS, 422, 2474
Giannios D., Uzdensky D.A., Begelman M.C., 2009, MNRAS, 395, L29
Hirose S., Krolik J.H., De Villiers J.-P., Hawley J.F., 2004, ApJ, 606, 1083
Guo F., Li H., Daughton W., Liu Y.-H. 2014, Phys. Rev. Lett., 113, 155005
Igumenshchev I.V., 2009, ApJ, 702, L72
Igumenshchev I.V., Narayan R., Abramowicz M.A., 2008, ApJ, 592, 1042
Kadowaki L.H.S., de Gouveia Dal Pino E.M., Singh C.B., 2015, ApJ, 802, 113
Karas V., Kopa'cek O., Kunneriath D., 2012, CQG, 29, 510

Koide S., Arai K., 2008, ApJ, 682, 1124
Kowal G., de Gouveia Dal Pino E.M., Lazarian A., 2011, ApJ, 735, 102
Kowal G., de Gouveia Dal Pino E.M., Lazarian A., 2012, Phys. Rev. Lett., 108, 241102
Kowal G., Falceta-Goncalves D.A., Lazarian A., Vishniac E.T., 2017, ApJ, 838, 91
Kowal G., Lazarian A., Vishniac E.T., Otamianowska-Mazur K., 2009, ApJ, 700, 63
Lazarian A., Vishniac E.T., 1999, ApJ, 517, 700
Lee H.K., Wijers R.A.M.J., Brown G.E., 2000, Phys. Rep., 325, 83
Machida M., Matsumoto R., 2003, ApJ, 585, 429
Lee H.K., Wijers R.A.M.J., Brown G.E., 2000, Phys. Rep., 325, 83
McKinney J.C., Narayan R., 2007, MNRAS, 375, 513
McKinney J.C., Tchekhovskoy A., Blandford R.D., 2012, MNRAS, 423, 3083
Meier D.L., 2012, Black Hole Astrophysics: The Engine Paradigm, Springer Verlag, Berlin Heidelberg
Narayan R., Igumenshchev I.V., Abramowicz M.A., 2003, PASJ, 55, L69
O'Riordan M., Pe'er A., McKinney J.C., 2016, ApJ, 819, 95
Parfrey K., Giannios D., Beloborodov, 2015, MNRAS, 446, 61
Semenov V.S., Dyadechkin S.A., Heyn M.F., 2014, Phys. Scr., 89, 045003
Singh C.B., de Gouveia Dal Pino E.M., Kadowaki L.H.S., ApJ, 799, L20
Singh C.B., Mizuno Y., de Gouveia Dal Pino E.M., ApJ, 824, 48
Sironi L., Spitkovsky A., ApJ, 783, L21
Takamoto M., Inoue T., Lazarian A., 2015, ApJ, 815, 16
Tchekhovskoy A., Narayan R., McKinney J.C., 2011, MNRAS, 418, L79
Werner G.R., Uzdensky D.A., 2017, ApJ, 843, L27
Werner G.R., Uzdensky D.A., Cerutti B., Nalewakjo K., Begelman M.C., ApJ, 816, L8
Yokosawa M., Ishizuka T., Yabuki Y., 1991, PASJ, 43, 427
Zenitani S., Hoshino M., 2008, ApJ, 677, 530
Zhang B., Yan H., 2011, ApJ, 726, 90

This paper has been typeset from a TEX/LATEX file prepared by the author.